

Photocurrent response of hydrogenated nanocrystalline silicon thin films

R. Zhang,^{a)} X. Y. Chen, K. Zhang, and W. Z. Shen^{b)}

Laboratory of Condensed Matter Spectroscopy and Opto-Electronic Physics, Department of Physics, Shanghai Jiao Tong University, 1954 Hua Shan Road, Shanghai 200030, People's Republic of China

(Received 31 May 2006; accepted 6 September 2006; published online 20 November 2006)

We report on the optoelectronic properties of the hydrogenated nanocrystalline silicon (nc-Si:H) thin film containing large density of nanometer grains and voids. By comparison with the bulk silicon, strong optical absorption and high photocurrent are found in the nc-Si:H thin film and attributed to the enhancement of the optical absorption cross section and good carrier conductivity in the nanometer grains and voids. The observed strong photocurrent signals can be well described by the extended diffusion-recombination model. The high photocurrent response may facilitate the fabrication of infrared photodetector by a single layer of nc-Si:H thin film on a glass substrate, which shows superiority to the traditional amorphous Si photodetector with a diode or Schottky-barrier structure constructed by multilayer films on the crystalline Si substrate. © 2006 American Institute of Physics. [DOI: 10.1063/1.2388042]

I. INTRODUCTION

The amorphous silicon (*a*-Si) material has attracted much attention for potential application in optoelectronic devices due to its merit of strong optical absorption. However, there is an unavoidable disadvantage in the *a*-Si thin films with high density of dangling bonds and midgap states, which strongly localize the free carriers and shrink the carrier lifetime. These factors result in a low efficiency of the free carrier production and therefore the energy conversion.¹ The hydrogenation of the *a*-Si to fabricate the hydrogenated *a*-Si (*a*-Si:H) thin films has been known to be a very good way to improve the carrier transport properties through the H atoms not only saturating the dangling bonds and degrading the charge-trapper density, which enhances the collection efficiency, but also forming short-range order (nanocrystallinity) that causes the *a*-Si:H to be a semiconductor material with higher carrier mobility. However, the photocurrent response of the *a*-Si:H is still not good enough for high performance optoelectronic devices due to its low conductance. Usually, *a*-Si:H thin films should be grown on crystalline silicon (*c*-Si) substrates to form Schottky-barrier or diode structures, where the *a*-Si:H film must be thin enough (less than 1 μm) to effectively collect the photogenerated carriers due to the short diffusion length and recombination time.

The recent investigations have shown that the hydrogenation under certain conditions could further induce the disorder-to-order structure transition, resulting in the formation of high density of nanocrystals in the *a*-Si thin films.² Generally, the hydrogenated nanocrystalline silicon (nc-Si:H) thin films are composed approximately of 50% Si nanocrystals (mean grain size 3–6 nm) and 50% *a*-Si tissues in the interface regions among the grains.³ The high density of nanometer grains in the nc-Si:H largely improves the structure order and impurity doping efficiency, resulting in a high con-

ductivity in the range of $\sim 10^{-2} - 10^2 \Omega^{-1} \text{cm}^{-1}$,³⁻⁵ much higher than that of *a*-Si or *a*-Si:H materials in the range of $\sim 10^{-8} - 10^{-4} \Omega^{-1} \text{cm}^{-1}$.^{6,7} The improved conductivity in the nc-Si:H thin films would also be advantageous to the photo-generated carrier collection, which leads to a wide potential optoelectronic applications with improved performance, such as the infrared detection and imaging devices.^{8,9}

In this paper, we report the optoelectronic properties of high-quality nc-Si:H thin films on glass substrates by plasma-enhanced chemical vapor deposition (PECVD). In combination with the x-ray diffraction (XRD), Raman, current-voltage (*I*-*V*), and Hall measurements to identify the structure and carrier transport properties of the nc-Si:H thin films, we have employed the optical transmission and photocurrent measurements to investigate the photogenerated carrier characteristics. We will show that the band-gap transition within the nanometer Si grains dominates the observed photocurrent response.

II. SAMPLE GROWTH AND STRUCTURAL CHARACTERIZATIONS

The nc-Si:H thin film samples were prepared in a radio frequency (13.56 MHz and power 60 W) capacitively coupled PECVD system from silane (SiH_4) and hydrogen (H_2) at a temperature of 250 °C and a chamber pressure of 1.0 Torr. The percentage content of silane ($\text{SiH}_4/\text{SiH}_4 + \text{H}_2$) is about 1.0%. The nc-Si:H thin film samples with a thickness of $\sim 1.0 \mu\text{m}$ were doped with phosphine (PH_3/SiH_4) of $\sim 0.8\%$ on the glass substrates. The deposition rate is as low as about 0.3 Å/s under the present hydrogen dilution, resulting in good quality and stability of the nc-Si:H film with hydrogen content of $\sim 5.0 \text{ at. } \%$ revealed by elastic recoil detection analysis.⁵ The structure of the nc-Si:H thin films has been characterized by XRD, Raman, and infrared transmission measurements, which were performed on a Bruker-axes D8Advance instrument in the standard θ - 2θ configuration, a Jobin Yvon LabRAM HR800 UV micro-Raman

^{a)}Also at Division of Basic Courses, Shanghai Maritime University, Shanghai 200135, People's Republic of China.

^{b)}Author to whom correspondence should be addressed; electronic mail: wzshen@sjtu.edu.cn

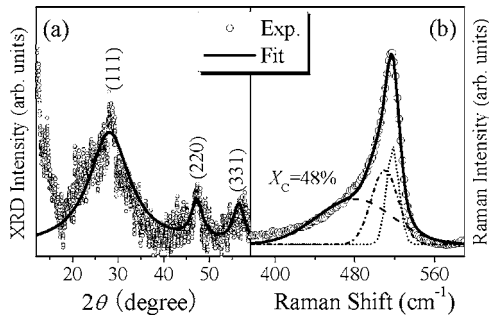


FIG. 1. (a) Experimental x-ray diffraction spectrum (circles) of the nc-Si:H thin film sample together with the Lorentzian fitting (solid curve) to the three diffraction peaks of (111), (220), and (331). (b) Experimental (circles) and fitted (solid curve) Raman spectra of the nc-Si:H thin film sample.

system in backscattering configuration (with a laser wavelength of 514.5 nm), and a Nicolet Nexus 870 Fourier transform infrared spectrometer, respectively.

Figure 1(a) presents the XRD results of a typical nc-Si:H sample (open circles) displaying two clear diffraction peaks of (111) and (220), together with a dim (331) peak of Si. Using Lorentzian fitting (solid curve) to the diffraction peaks as well as the Scherrer formula,¹⁰ we can obtain the average grain sizes of Si nanocrystals $D_{(220)}$ of 2.9 nm. It should be noted that the appreciable low-angle scattering in the range of $2\theta < 15^\circ$ is indicative of the actual nanometer-sized voids within the nc-Si:H thin film.¹¹ In addition, the Raman scattering data (open circles) in Fig. 1(b) clearly exhibit the typical asymmetric peak, involving the contribution from both the Si nanocrystals at ~ 510 – 520 cm^{-1} and the amorphous phase at ~ 480 cm^{-1} . For the determination of the crystalline fraction X_C , the Raman spectrum is decomposed into three Gaussian phonon bands with peaks at 480 cm^{-1} (dashed curve), 510 cm^{-1} (dash-dotted curve), and 518 cm^{-1} (dotted curve). X_C of 48% is then obtained from the ratio of the integrated intensity of the Gaussian bands centered at 510 and 518 cm^{-1} to the total integrated intensity of the three bands.¹²

III. THEORETICAL BACKGROUND

For a photoconductive semiconductor illuminated by light, the photoexcited carrier pairs will diffuse and recombine to produce photocurrent. Within the constraints of the drift-diffusion approximation, carrier transport in the photoconductive semiconductor can be completely described by the equations of carrier diffusion, charge conservation, and current continuity. By solving these equations, we can obtain the photoexcited excess carriers Δn along the light incident direction (x) as^{13–15}

$$\Delta n(x) = C \exp\left(\frac{x}{L_D}\right) + B \exp\left(-\frac{x}{L_D}\right) + \frac{g(x)\tau}{1 - \alpha^2 L_D^2}, \quad (1)$$

where C and B can be determined by the boundary conditions assuming that the recombination at each surface occurs at the same rate. References 14 and 15 have presented the detailed expressions of C and B as the functions of the thin film thickness d , optical absorption coefficient α , volume recombination lifetime τ , bulk ambipolar diffusion length

L_D , and surface recombination velocity S . In the case of $\alpha d \gg 1$ without the optical multireflection in the specimen, the generation ratio of the photoexcited excess carriers $g(x)$ can be expressed as $g(x) = \alpha(1-R)\exp(-\alpha x)$ with the reflectivity R . However, the optical multireflection usually cannot be neglected due to the relatively weak absorption in semiconductor thin films, which will result in the modification of the generation ratio as¹³

$$g(x) = \alpha(1-R) \frac{\exp(-\alpha x) + R \exp(-2\alpha d)\exp(\alpha x)}{1 - R^2 \exp(-2\alpha d)}. \quad (2)$$

The corresponding photocurrent in semiconductor thin films after the consideration of both the optical multireflection and the surface recombination can be written as

$$I_{PC} \propto \int_0^d \Delta n(x) dx \propto \gamma \frac{1-R}{1 - \alpha^2 L_D^2} \times \left[1 - e^{-\alpha d} - \frac{\alpha L_S(1 + e^{-\alpha d}) + \alpha^2 L_D^2(1 - e^{-\alpha d})}{1 + (L_S/L_D)\coth(d/2L_D)} \right], \quad (3)$$

where $\gamma = (1 + R e^{-\alpha d}) / (1 - R^2 e^{-2\alpha d})$ and $L_S = S\tau$ relates the carrier flux at the interface to the excess carrier concentration. In the case of $\alpha d \gg 1$, the factor γ due to the multireflection approaches a constant and Eq. (3) returns to the previous results in Refs. 13 and 14.

As well known, the interband and bandtail transitions dominate the optical absorption in the nc-Si:H thin film due to the short-range-ordered and long-range-disordered structures. Therefore, the following expression is usually applied to describe the real optical absorption coefficient α of indirect band-gap semiconductors¹⁶ such as nc-Si:H,

$$\alpha(E) = \begin{cases} \alpha_0 \exp[E/E_u] & E \leq E_t, \\ B_0(E - E_g)^2/E & E > E_t, \end{cases} \quad (4)$$

where α_0 and B_0 are constants independent of the photon energy E , E_g is the optical band-gap energy, E_t and E_u could be interpreted as characteristic energies of the distribution of electronic states in bandtaillike regions. Usually, the optical absorption coefficient can be obtained from the optical transmission or reflection spectra. The optical constants of the nc-Si:H thin film can be expressed as

$$N_f = n_f + ik_f. \quad (5)$$

The imaginary part of the complex refractive index k_f is related to α by $k_f = \lambda \alpha / 4\pi$. For the dispersion of the nc-Si:H refractive index n_f , we use a modification of the Sellmeier formula suggested by Herzberger, $n_f = n_A + n_B / (\lambda^2 - 0.028)$, where λ is the wavelength in micrometers, n_A and n_B are the material constants determined by optical transmission experiments.

As demonstrated in the low-angle XRD results of Fig. 1(a), the nanometer voids at the surface and grains in the volume of the 1- μm -thick nc-Si:H thin film would also have an effect on the optical results, which should be taken into account in the calculation. The root-mean-square (rms) roughness σ of these inhomogeneous voids and grains in the nc-Si:H thin film is about a few tens of nanometers, far

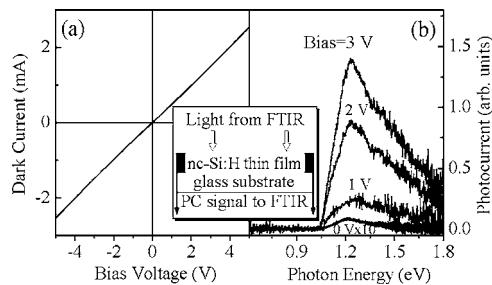


FIG. 2. Room-temperature (a) dark current-voltage characteristics of the nc-Si:H thin film sample and (b) photocurrent spectra of the nc-Si:H thin film sample measured under various bias voltages. The inset shows the configuration for the photocurrent measurements.

shorter than the light wavelength at the optical band-gap energy, where the optical reflection and transmission can be described by the light scattering factors Sc within the scalar theory. Thus, the Fresnel coefficients for amplitudes of reflected (r_{12}) and transmitted (t_{12}) lightwave at the rough interface between media 1 and 2 can be simply expressed as¹⁷

$$r_{12} = \frac{n_1 - n_2}{n_1 + n_2} Sc^r_{12} = \frac{n_1 - n_2}{n_1 + n_2} \exp \left[-\frac{1}{2} \left(\frac{4\pi n_1 \sigma}{\lambda} \right)^2 \right],$$

$$t_{12} = \frac{2n_1}{n_1 + n_2} Sc^t_{12} = \frac{2n_1}{n_1 + n_2} \exp \left\{ -\frac{1}{2} \left[\frac{2\pi(n_1 - n_2)\sigma}{\lambda} \right]^2 \right\}, \quad (6)$$

where σ is the rms surface roughness between the media 1 and 2 with their corresponding refractive indices n_1 and n_2 . Given the nc-Si:H thin film grown on a nonabsorbing substrate with a corresponding refractive index n_s [for the glass substrate $n_s = 1.55$ (Ref. 18)], we can obtain the optical transmission of the thin film from Eqs. (4)–(6). Through fitting the experimental transmission spectra, we will have the important optical parameters, such as the band-gap energy E_g , rms surface roughness σ , and absorption coefficient α . Following this fitting procedure, we can further get the bulk ambipolar diffusion length L_D and surface recombination length L_S by calculating the photocurrent with Eq. (3).

IV. RESULTS AND DISCUSSIONS

We start with the electrical transport measurements of the dark I - V and Hall experiments. In these electrical experiments, indium has been employed as the contact material. Figure 2(a) shows the room-temperature dark I - V characteristics measured with a computer-controlled Keithley 2400 source meter. The linear shape of the I - V curve for the sample with coplanar electrodes demonstrates that indium is a good Ohmic contact material for the nc-Si:H thin films. The Hall measurements under a standard Van der Pauw configuration show its room-temperature conductivity of $3.6 \Omega^{-1} \text{cm}^{-1}$ (with an electron mobility of $0.13 \text{cm}^2/\text{Vs}$ and an electron concentration of $1.9 \times 10^{20} \text{cm}^{-3}$). As demonstrated in the structural characteristics of Fig. 1, it is the formation of high density nanocrystals that results in the much higher conductivity in nc-Si:H than that of a -Si:H (below $10^{-4} \Omega^{-1} \text{cm}^{-1}$).⁶ The improvement of conductivity will be certain to improve the photogenerated carrier collection efficiency.

On the basis of the good and stable electrical contacts between the indium and the nc-Si:H thin films, the photocurrent measurements have been carried out on a Nicolet Nexus 870 Fourier transform infrared spectrometer calibrated by a DTGS TEC detector. Two Ohmic contacts are formed on the nc-Si:H thin film in the size of about 4.0mm^2 and 1.0mm in distance, as illustrated in the inset of Fig. 2. Usually, the free carrier concentration increases in the semiconductor due to the photogenerated carriers. Under a fixed external voltage, the resultant photocurrent signal increases with the photon energy below a threshold due to the increased optical absorption, but decreases above the threshold due to the recombination of the photogenerated carriers caused by the extremely strong optical absorption. These two inverted processes often result in the appearance of a photocurrent peak, as clearly observed in Fig. 2(b).

Figure 2(b) presents four room-temperature photocurrent spectra of the nc-Si:H thin film sample measured under a series of applied biases. The experimental photocurrent signal is very small at zero bias, but increases rapidly with the applied bias, indicating that the external field is helpful for improving photocurrent signal due to the enhancement of the free photocarrier generation and transport. The process of free photocarrier generation should start with the absorption of light to form an exciton state in grains where the electron-hole pairs are bound together, and then the external electric field separates these bound electron-hole pairs into free carriers.¹ In the nc-Si:H thin film, the external field not only helps the free photocarrier generation, but also enhances the photocarrier hopping through the boundaries by increasing the tunneling probability. Therefore, the observed photocurrent in the nc-Si:H thin film is a result of field-assisted carrier generation and hopping transport,^{9,19} and we can attribute the photocurrent to be the multiple tunneling and/or hopping transports of the dissociated electron-hole pairs within the grains under the external bias.

Furthermore, the process of free carrier generation due to the absorption of light to form an exciton state within grains is demonstrated by the photon energy dependence of the experimental photocurrent spectra. As clearly observed in Fig. 2(b), the experimental photocurrent begins with the photon energy of 1.05eV , which is very close to that of c -Si ($\sim 1.08 \text{eV}$) at room temperature. This characteristic of optical absorption is associated with the crystallites contained within the thin film, as revealed in the XRD and Raman results above. The photocurrent signal below 1.05eV , as a result of the transitions from the dominant deep defect band and the bandtail region in the a -Si:H boundaries, becomes very weak and hard to be distinguished from the noise signals. It should be noted that the strong photocurrent signals in the photon energy range from 1.05 to 1.50eV are a result of the band-gap transition occurring in the photon energy below the a -Si:H band gap ($\sim 1.70 \text{eV}$), with a threshold energy of 1.05eV due to the nanometer Si grains in the thin film.^{17,20} Although the photon energy threshold of the band-gap transition within the grains is nearly the same as that of the bulk Si materials, they take on quite different behaviors, as discussed below.

Figure 3 presents the enlargement of the photocurrent

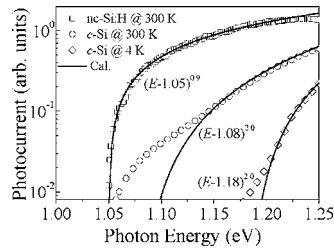


FIG. 3. Experimental photocurrent spectra of the nc-Si:H and *c*-Si from Ref. 19. The scatters and solid curves represent the experimental and calculated results, respectively.

spectrum under a bias voltage of 3 V for the nc-Si:H, as well as a comparison with the results of *c*-Si from Ref. 19. In the weak absorption regime near the band edge ($\alpha \rightarrow 0$), Eq. (3) can be simplified as $I_{PC} = \alpha[d - 2L_S / (1 + L_S \coth(d/2L_D)/L_D)]$, indicating that the photocurrent is directly proportional to the strength of optical absorption. As well known, the phonon-assisted transition absorption plays an important role in the indirect gap materials of *c*-Si, resulting in the increase of the photocurrent with the temperature. In the band-gap transition, the absorption coefficient near the band edge can be simply expressed as $\alpha(E) = A(E - E_g)^x$ with constant A , where the power number x is 0.5 for direct band-gap and 2.0 for indirect band gap. The fitted curve in Fig. 3 reveals that the power number x is 2.0 for the *c*-Si but 0.9 for the nc-Si:H. In addition, the photocurrent of the nc-Si:H thin film shows a rapid increase by two orders of magnitude at the sub-band-gap energy edge, even higher than that of *c*-Si. The strong optical absorption can be explained by the destroy of the crystal moment and symmetry selection rules in the phonon-assisted band-gap transition due to the loss of translational symmetry at the grain boundaries. In fact, the high density nanometer voids, as evidenced by the appreciable low-angle scattering in Fig. 1(a), enlarge the surface-to-volume ratio in the nc-Si:H thin film, improving the optical absorption cross section. These factors play important roles in the enhancement of optical absorption, and therefore high photocurrent and power number x approaching 0.5 in the nc-Si:H thin film.

Nevertheless, it should be noted that the voids in the *a*-Si:H boundaries have a double effect on the photocurrent: advantageous to the optical absorption but disadvantageous to the photocarrier transport. As shown in Fig. 3, the optical absorption and performance of photocurrent response increase with the presence of the voids and *a*-Si boundaries. However, too much volume fraction of voids and *a*-Si component would reduce the carrier free path and degrade the performance of photocurrent response despite of the enhancement of the optical absorption. The nc-Si:H thin film with about 50% crystalline fraction, where the voids do not heavily prevent the carrier transport due to its nanometer size near to the electron wavelength, may be an optimal case for the highest photocurrent in the silicon-based materials. In this case, the optical absorption quickly becomes strong with an increase of photon energy as observed above. Once the photon energy is beyond the band gap, the strong optical absorption increases not only the excessive carrier density but also the recombination rate, especially on the thin film

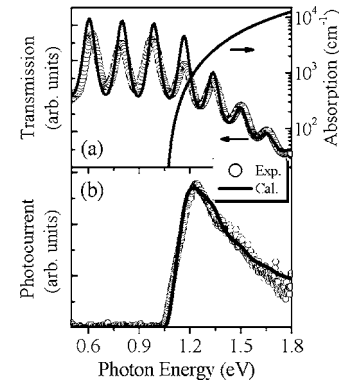


FIG. 4. (a) Optical transmission and absorption and (b) photocurrent spectrum of the nc-Si:H thin film under 3 V bias voltage. The circles and solid curves represent the experimental and calculated results, respectively.

surface. At the same time, the transmission of the thin film also decreases rapidly, as demonstrated by the following transmission results.

Figure 4(a) shows the experimental room-temperature spectrum of the nc-Si:H sample (open circles). The interference fringes are clearly observed below the photon energy of ~ 1 eV, above which the transmission decreases with the increase of photon energy. Obviously, it is the above band-gap transition within the grains that results in the strong optical absorption and weak transmission. Using Eqs. (4)–(6) in Sec. III, we can further extract the optical absorption information in nc-Si:H by fitting the experimental transmission data. Solid curve in Fig. 4(a) is the calculated result, which gives the band-gap energy of 1.05 eV, in good agreement with the photocurrent results of Ref. 20. The yielded optical absorption has also been shown in Fig. 4(a), which is basically in the same order as the reported results from hydrogenated microcrystalline silicon thin films by Poruba *et al.*¹⁷ and Vanček and Poruba.²¹ In addition, the obtained rms surface roughness σ of 20 nm also reflects well the average size of *a*-Si boundaries and *c*-Si grains in the nc-Si:H thin film.

In combination with the above extracted optical absorption results, we have employed the extended theory for the photogenerated carriers and their recombination at the surface [Eq. (3)] to explain and simulate the observed photocurrent spectrum in nc-Si:H. Figure 4(b) presents the experimental and calculated results of the photocurrent spectra at a bias voltage of 3 V, where a good agreement is achieved. In the calculation, the band gap E_g in the optical absorption is 1.05 eV and the diffusive constant L_D is 170 nm, consistent with the reported results in the hydrogenated microcrystalline silicon thin films.^{6,22} Furthermore, the obtained result of $L_S = 15L_D$ indicates that the surface recombination rate is very high, resulting in a quick degradation of the photocurrent at high photon energy side. Similar results have also been observed in Refs. 13 and 15.

Finally, we investigate the dependence of the optical transmission and photocurrent signal on the film thickness, where the optical and diffusion constants are independent of the thickness of the nc-Si:H thin film. Figure 5 shows the calculated transmission and photocurrent spectra for three different thicknesses of 0.5, 1.0, and 2.0 μm . With the in-

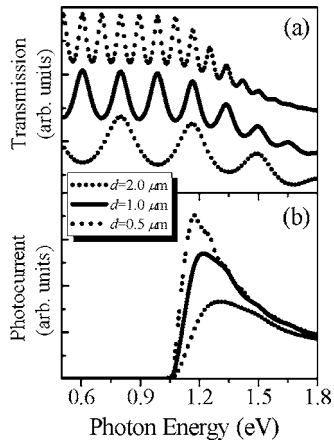


FIG. 5. Theoretical (a) transmission and (b) photocurrent spectra of the nc-Si:H thin film with different thicknesses of 0.5 (dashed curve), 1.0 (solid curve), and 2.0 μm (dotted curve).

crease of thickness d , the interference fringe becomes dense and weak in the regime above the band gap due to the increase of optical absorption, as already observed in the experiments of the a -Si:H thin films.²³ Accordingly, the photocurrent signal increases due to the increase of photoexcited electron-hole pairs. Moreover, the photocurrent response at the low energy side can be effectively enhanced by increasing the thin film thickness, while the high energy side photocurrent is basically independent of the thickness, because the photons with high energy are absorbed mostly at the surface and cannot effectively contribute to photocurrent. Therefore, the photocurrent peak will shift to lower energy with the increase of thin film thickness, and the interference fringe may appear in the photocurrent spectra when the thin film thickness is about several microns. In addition to the thickness, the transmission and photocurrent in the nc-Si:H thin films also strongly depend on the growth conditions, which are critical to the microstructure of the thin films.

V. CONCLUSIONS

We have demonstrated that the band-gap transition occurring within the grains dominates the optical absorption and photocarrier generation under the electric field in the nc-Si:H thin films through the photocurrent and optical transmittance experiments, together with the structural characterizations by XRD and Raman. These experimental results show that the formation of nc-Si:H thin film with high density of nanometer grains and voids is an effective way to improve the photogenerated carrier collection efficiency and enhance the photocurrent response through the increase in

the conductivity and optical absorption cross section. The nanometer grains and voids in the nc-Si:H thin film have an ability to optimize the photocurrent response, even higher than that in bulk c -Si. The observed high photocurrent response in the nc-Si:H thin films grown on the glass substrates can be expected to be applied on the commercial optoelectronic devices with high performance and low cost.

ACKNOWLEDGMENTS

This work is supported by the Natural Science Foundation of China under contract Nos. 10125416, 60576067, and 10674094, the National Minister of Education Program for Changjiang Scholars and Innovative Research Team in University (PCSIRT), and the Shanghai Municipal Commission of Science and Technology Project [Nos. 05DJ14003 05QMH1411, and 06JC14039] as well as the excellent young teachers plan (No. 025063) at Shanghai Maritime University. The authors would like to thank H. Chen and Professor Y. L. He for their valuable discussion.

- ¹R. S. Crandall, R. Williams, and B. E. Tompkins, *J. Appl. Phys.* **50**, 5506 (1979).
- ²J. Koh, A. S. Ferlauto, P. I. Rovira, C. R. Wronski, and R. W. Collins, *Appl. Phys. Lett.* **75**, 2286 (1999).
- ³Y. L. He, G. Y. Hu, M. B. Yu, M. Liu, J. L. Wang, and G. Y. Xu, *Phys. Rev. B* **59**, 15352 (1999).
- ⁴S. C. Saha and S. Ray, *J. Appl. Phys.* **78**, 5713 (1995).
- ⁵X. Y. Chen, W. Z. Shen, and Y. L. He, *J. Appl. Phys.* **97**, 024305 (2005); M. H. Gullanaar, H. Chen, W. S. Wei, R. Q. Cui, and W. Z. Shen, *ibid.* **95**, 3961 (2004).
- ⁶R. Brüggemann, J. P. Kleider, C. Longeaud, D. Mencaraglia, J. Guillet, J. E. Bourée, and C. Niikura, *J. Non-Cryst. Solids* **266–269**, 258 (2000).
- ⁷M. H. Brodsky, R. S. Title, K. Weiser, and G. D. Pettit, *Phys. Rev. B* **1**, 2632 (1970).
- ⁸M. Tucci and R. DeRosa, *Solid-State Electron.* **44**, 1315 (2000).
- ⁹H. Mimura and Y. Hatanaka, *J. Appl. Phys.* **61**, 2575 (1987).
- ¹⁰M. R. Fitzsimmons, J. A. Eastman, M. Müller-Stach, and G. Wallner, *Phys. Rev. B* **44**, 2452 (1991).
- ¹¹S. C. Moss and J. F. Graczyk, *Phys. Rev. Lett.* **23**, 1167 (1969).
- ¹²I. Kaiser, N. H. Nickel, W. Fuhs, and W. Pilz, *Phys. Rev. B* **58**, R1718 (1998).
- ¹³S. C. Shen, *Scpectroscopy and Optical Properties of Semiconductors* (Scientific, Beijing, 2002).
- ¹⁴H. B. DeVore, *Phys. Rev.* **102**, 86 (1956).
- ¹⁵K. Lefki and P. Muret, *J. Appl. Phys.* **74**, 1138 (1993).
- ¹⁶A. S. Ferlauto, G. M. Ferreira, J. M. Pearce, C. R. Wronski, R. W. Collins, X. M. Deng, and G. Ganguly, *J. Appl. Phys.* **92**, 2424 (2002).
- ¹⁷A. Poruba *et al.*, *J. Appl. Phys.* **88**, 148 (2000).
- ¹⁸A. R. Forouhi and I. Bloomer, *Phys. Rev. B* **38**, 1865 (1988).
- ¹⁹T. P. Pearsall *et al.*, *Phys. Rev. B* **57**, 9128 (1998).
- ²⁰D. Kwon, C. C. Chen, J. D. Cohen, H. C. Jin, E. Hollar, I. Robertson, and J. R. Abelson, *Phys. Rev. B* **60**, 4442 (1999).
- ²¹M. Vaněček and A. Poruba, *Appl. Phys. Lett.* **80**, 719 (2002).
- ²²R. Brüggemann, *J. Appl. Phys.* **92**, 2540 (2002).
- ²³M. Vaněček, J. Kočka, A. Poruba, and A. Fejfar, *J. Appl. Phys.* **78**, 6203 (1995).